EDGE ARTICLE

Check for updates

High-throughput encapsulated nanodroplet screening for accelerated co-crystal discovery†

Jessica P. Metherall, [ID] [a] Philip A. Corner, [ID] [b] James F. McCabe, [ID] [b] Michael R. Probert [ID] [a] and Michael J. Hall [ID] *[a]

Co-crystals are composed of two or more chemically inequivalent molecular species, excluding solvents, generally in a stoichiometric ratio. Co-crystals are particularly important in pharmaceutical development, where a suitable co-crystal can significantly improve the physiochemical and pharmacokinetic properties of an active pharmaceutical ingredient. However, co-crystal discovery remains both practically challenging and resource intensive, requiring the extensive searching of complex experimental space. Herein, we demonstrate a high-throughput (HTP) nanoscale co-crystallisation method for the rapid screening of large areas of co-crystallisation space with minimal sample requirements, based on Encapsulated Nanodroplet Crystallisation (ENaCt). HTP co-crystallisation screening by ENaCt allowed rapid access to all 18 possible binary co-crystal combinations of 3 small molecules and 6 co-formers (A/B), through the use of 3456 individual experiments exploring solvent, encapsulating oil and stoichiometry, including 10 novel binary co-crystal structures elucidated by single crystal X-ray diffraction (SCXRD). Higher-order co-crystal (HOC) discovery, accessing co-crystals containing three or more molecules, is one of the most challenging co-crystal research areas, due to the highly complex experimental landscape that must be navigated. Herein, we further exemplify the power of ENaCt co-crystallisation by application to HOC discovery. HTP ENaCt co-crystallisation screening of three component (A/B/C) and four component (A/B/C/D) combinations gave ready access to both ternary and quaternary HOCs, each containing three or four different molecular species respectively. In total, 13 056 individual ENaCt experiments are presented resulting in 54 co-crystal structures by SCXRD, including 17 novel binary co-crystals, 8 novel ternary co-crystals and 4 novel quaternary co-crystals. ENaCt co-crystallisation is thus demonstrated to be a highly impactful and efficient tool in the search for small molecule co-crystals, through the employment of parallelised HTP nanoscale experimental workflows.

Introduction

A co-crystal can be defined as a crystalline solid containing two or more chemically inequivalent molecules, generally, present in a stoichiometric ratio, and excluding simple salts or solvates.[1] Co-crystals have altered physiochemical properties in comparison to a simple mixture of crystals of the individual components, and this effect has been exploited in many research areas, including supramolecular and functional materials,[2] pigments,[3] agrochemicals,[4] energetic materials[5] and

[a]Chemistry, School of Natural and Environmental Sciences, Newcastle University, Newcastle upon Tyne, UK. E-mail: michael.hall@newcastle.ac.uk

[b]Early Product Development & Manufacturing, Pharmaceutical Sciences, BioPharmaceuticals R&D, AstraZeneca, Macclesfield, UK

particularly pharmaceuticals.[6] In the case of pharmaceuticals, the differing physical properties of a co-crystal containing an active pharmaceutical ingredient (API) are commonly used during formulation to improve stability and bioavailability,[7] and API co-crystal forms can be a key element of associated intellectual property.[8]

Due to the importance of small molecule co-crystals, considerable effort has been devoted to their discovery using both classical and modern crystallisation methods, including neat and liquid-assisted grinding,[9] melt microdroplets,[10] laser irradiation of mixed powders,[11] sonocrystallisation,[12] and heteronuclear seeding.[13] These experimental efforts are typically supported with empirical and experimentally driven crystal engineering methods,[14] particularly the use of supramolecular synthons,[15] and increasingly paired with computational methods for co-crystal predication and design.[16]

However, successful crystallisation of multi-component systems still remains experimentally challenging, due to the large number of experimental variables that must be explored. The rigorous exploration of such a large experimental landscape

for a molecule of interest is thus best attempted through high-throughput (HTP) approaches.[17] Despite considerable advances in the area,[18] state-of-the-art HTP co-crystal screening for small molecules still requires access to gram quantities of substrate, with milligrams of material used per experiment. In addition, experimental read-outs are typically reliant on Raman spectroscopy and/or powder X-ray diffraction to identify the presence of new crystal forms, with follow-up crystal growth and single crystal X-ray diffraction (SCXRD) needed to validate hits. Thus, particularly with sample limited material, only a partial exploration of the available experimental space is performed. Recently, we have developed Encapsulated Nanodroplet Crystallisation (ENaCt) as an HTP crystallisation platform for small molecules.[19] ENaCt employs liquid handling robotics to set-up nanolitre scale crystallisation experiments in 96-well plate format, in which solutions of test molecules in organic solvents are encapsulated in inert oils to mediate the rate of sample concentration, through both evaporation and/or diffusion into the oil. This facilitates large scale, parallel, crystallisation screening using a few micrograms of material per experiment, allowing hundreds of experiments to be undertaken with only milligrams of substrate. Over a number of days, slow growth of suitable single crystals occurs, and crystallisation outcomes can be assessed by SCXRD, resulting in full structural characterisation of crystal forms obtained. ENaCt has proven extremely successful in exploring crystallisation space for single-component systems, allowing for the study of a wide range of small molecule classes as well as hydrogen-bonded organic frameworks (HOFs),[20] but has not been applied previously to multi-component crystal systems.

Our aim was therefore to develop HTP ENaCt protocols suitable for extensive exploration of the co-crystallisation space for small molecules. We anticipated that ENaCt would enable 1000s of co-crystallisation experiments to be performed in parallel, with minimal sample requirements, generating co-crystals suitable for SCXRD analysis. This approach would provide a step-change in co-crystal screening allowing rapid access to new, structurally characterised, co-crystals.

Herein, we report our development of new approaches for co-crystallisation *via* ENaCt, and their application to co-crystal discovery. Following a demonstration of exhaustive co-crystal screening for a series of binary co-crystals, allowing access to all eighteen of the possible binary combinations of three molecules with six different co-formers, we have expanded our approach to encompass the more challenging problem of accessing higher-order co-crystals (HOCs), with the subsequent discovery of eight new ternary and four new quaternary HOCs.

Results and discussion

Binary co-crystals

We commenced our study by focussing on the development of HTP ENaCt methods for the discovery of binary co-crystals, as these systems are of most interest in industrial applications for the formulation of APIs.

For our initial co-crystallisation experiments we selected 4,4′-bipyridine **1**, caffeine **2** and nicotinamide **3** as test substrates.

These molecules were chosen as a test set as their co-crystallisation has been studied by multiple groups, thus the experimental landscape is well known and we hypothesised that any 'missing' combinations with simple co-formers are likely to have been previously attempted by classical methods, albeit not successfully.[9b,21] All three molecules are also aromatic, of similar molecular size, and contain one or more basic sp^2 hybridised nitrogen atoms capable of acting as H-bond acceptors. A set of six commonly used co-formers was also chosen, 2,4-dihydroxybenzoic acid **4**, 3,5-dinitrobenzoic acid **5**, glutaric acid **6**, 3-hydroxy-2-naphthoic acid **7**, methyl gallate **8**, and quinol **9**, all of which contained complementary functional groups capable of acting as H-bond donors, whilst also representing a range of different structural motifs (Fig. 1). Of the eighteen possible binary combinations of substrate and co-former, twelve were known in the literature (ESI, S4.5†). All eighteen combinations of substrates and co-formers were examined using the CSD Molecular Complementarity Tool (MCT), to assess the likelihood of co-crystal formation through analysis of five key molecular descriptors.[22] For substrate/co-former combinations known to form binary co-crystals, as well six previously unknown co-crystals, MCT gave uniformly high hit rates, suggesting that all combinations should be accessible.

Following preliminary solubility testing, the three substrates and six co-formers were independently crystallised as single component systems over 14 days using a standardised ENaCt screening protocol (288 experiments/3× 96-well plates, 12 solvents, 4 encapsulating oils (ESI, S3.2†)). This was to assist in both co-crystallisation solvent selection, and co-crystal identification during subsequent co-crystallisation screening experiments through comparative unit cell analysis. Crystals suitable
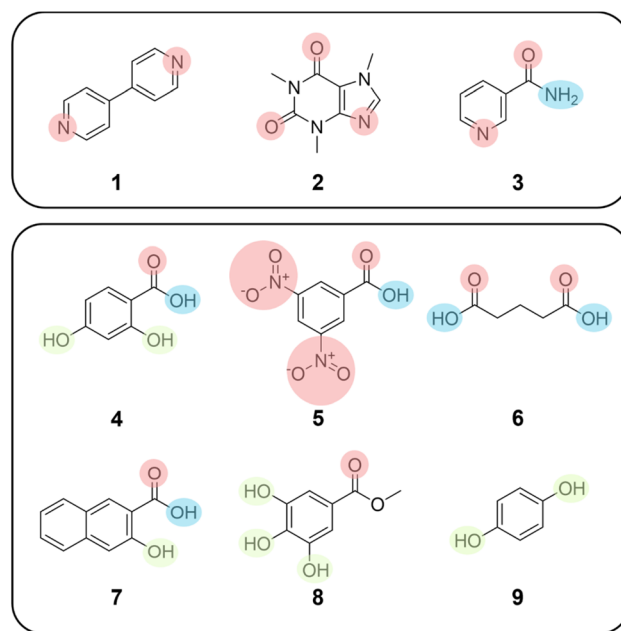

Fig. 1 Substrates and co-formers chosen for binary co-crystal screening, showing H-bond acceptor sites (red), H-bond donor sites (blue), and H-bond donor/acceptor sites (green).

for SCXRD were obtained for all six co-formers and two substrates, 4,4′-bipyridine **1** and nicotinamide **3**, in each case matching known crystal forms (ESI, S4.3†).

Based on these results, we selected four solvents (MeOH, DMF, MeNO$_2$ and 1,4-dioxane) to be used in subsequent co-crystal screening, chosen as both substrates and co-formers showed good solubility therein and represented a range of common solvent properties (ESI, S3.1†). In each case, stock solutions of both substrate and co-former were prepared near to the solubility limit for each compound/solvent combination.

ENaCt co-crystallisation experiments employed 200 nL of each of the four encapsulation oils dispensed across a 96-well glass plate, and 150 nL of each test solution, containing both substrate and co-former in a single solvent. Following set-up, plates were sealed with a glass cover slip and left for 14 days. Substrate/co-former solutions were examined in three different volume ratios (2 : 1, 1 : 1 and 1 : 2).

Note that inclusion of crystallisation experiments in which the ratio of substrate to co-formers is varied is important, as a pair of molecules can form multiple co-crystal forms with different substrate/co-former stoichiometries, and the stoichiometry of the co-crystal obtained does not necessarily match with the stoichiometry of the solution from which it was formed.[23]

ENaCt screening of all eighteen substrate/co-former combinations, with four different solvents, four different encapsulating oils (as well as no-oil controls) and three different substrate/co-former ratios, resulted in a total of 3456 individual crystallisation experiments including replicates, each employing a few micrograms of material, encompassing 1080 different crystallisation conditions. Through the use of HTP liquid handling robotics, targeted crystallisation screening experiments can be set up in a short space of time, taking less than an hour to prepare for each substrate/co-former system.

After 14 days, all experiments within the 96-well plates were inspected by cross-polarised optical microscopy to search for successful crystallisation outcomes. Crystals were extracted from the 96-well plates and examined by SCXRD. A number of single-component crystals of either substrate or co-former were identified, which were differentiated from target co-crystals by both crystal morphology and unit-cell data (ESI, S4.4.1†). For every one of the eighteen binary combinations of substrate and co-former, suitable co-crystals were obtained, and complete structural analysis was undertaken by SCXRD. Alongside the 13 known co-crystals obtained, we report the discovery of 10 new binary co-crystals, including examples of all 6 of the previously unreported substrate/co-former combinations, as well as new co-crystal solvates, hydrates, solvate/hydrates and stoichiometries (Fig. 2).

Of the new binary co-crystals obtained, the previously unreported combination of 4,4′-bipyridine **1** : methyl gallate **8** gave three related co-crystals, a 2 : 2 trihydrate, a 3 : 2 DMF solvate dihydrate and a 3 : 2 MeNO$_2$ disolvate dihydrate (ESI, S4.4.1†). The structure of the 4,4′-bipyridine **1** : methyl gallate **8** 2 : 2 trihydrate co-crystal is composed of 4,4′-bipyridine molecules held together by face-to-face π-interactions, where the nitrogen atoms form H-bonds to water and methyl gallate **8**, themselves

forming a linear H-bonded network co-planar to the crystallographic (−120) plane (Fig. 3A). Whilst the 3 : 2 DMF solvate dihydrate and the 3 : 2 MeNO$_2$ disolvate dihydrate show a related packing arrangement, with a trimeric π-stacked 4,4′-bipyridine unit H-bonded to a linear H-bond networked chain of water and methyl gallate molecules (Fig. 3B and C).

Two new 4,4′-bipyridine **1** co-crystals were also observed with both 3,5-dinitrobenzoic acid **5** and with 3-hydroxy-2-naphthoic acid **7**, in which the respective molecular stoichiometries (1 : 1 and 1.5 : 1, substrate : co-former) differed from those previously reported.

ENaCt co-crystallisation screening with caffeine **2** gave new co-crystals for both previously unreported small molecule/co-former pairings with 3,5-dinitrobenzoic acid **5** and quinol **9**, which were formed with 2 : 2 and 1.5 : 1 stoichiometries respectively.

Finally, the previously unreported combinations of nicotinamide **3** with methyl gallate **8**, quinol **9** and 3,5-dinitrobenzoic acid **5** were all obtained, formed with 1 : 1, 2 : 0.5 and 2 : 2 (MeOH disolvate) stoichiometries respectively.

Due to our success in accessing the target of binary co-crystals for all the possible 18 substrate/co-former combinations, via rapid, small scale, parallelised ENaCt co-crystallisation experiments, we next turned our attention to the much more challenging area of multi-component co-crystals which contain two or more co-formers.

Higher order co-crystals – ternary co-crystals

Although the primary focus of pharmaceutical co-crystal research revolves around the discovery of binary co-crystals, there is emerging interest in accessing multi-component or higher-order co-crystals (HOCs), in which three or more different small molecules are combined in a crystal, in stoichiometric ratios. Relatively few ternary and quaternary co-crystal are known, with around 150 ternary co-crystals and around 50 quaternary co-crystals reported prior to this work.[24,25] The comparatively small number of reported HOCs is due to added difficulties of exploring an increasingly complex experimental solid-state landscape, involving three or more molecular components alongside other experimental variables. Additionally, whilst crystal structure prediction (CSP) tools have become increasingly widespread for the rational design of binary co-crystals,[16a,18b,26] such a computational toolkit for the construction of HOCs is not well-established. Current HOC design strategies therefore mainly rely on the use of empirical crystal engineering approaches, based on supramolecular synthons,[15a,27] including synthon hierarchy,[28] shape-size mimicry[29] in combination with a long-range synthon Aufbau module (LSAM) strategy,[30] structural inequivalence,[31] and combinatorial synthesis.[32]

We envisaged that the combination of high-throughput ENaCt co-crystal screening with suitable crystal engineering strategies would enable us to efficiently access new ternary HOCs. To this end we designed a HOC ENaCt co-crystal screen in which the co-crystallisation of three different molecular

Fig. 2 Binary co-crystals accessed *via* ENaCt screening, including previously known co-crystals (white), new co-crystals (red), new co-crystal solvates, hydrates and solvate/hydrates (blue) and new co-crystals showing altered stoichiometry (green). CSD refcode (for known co-crystals), crystal composition ((A/B) : (solvent) : (water)), ENaCt crystallisation conditions (solvent, v/v ratio, oil) shown (MO = mineral oil, PDMSO = poly(dimethylsiloxane), FY = Fomblin YR-1800, and FC-40: Fluorinert FC-40).
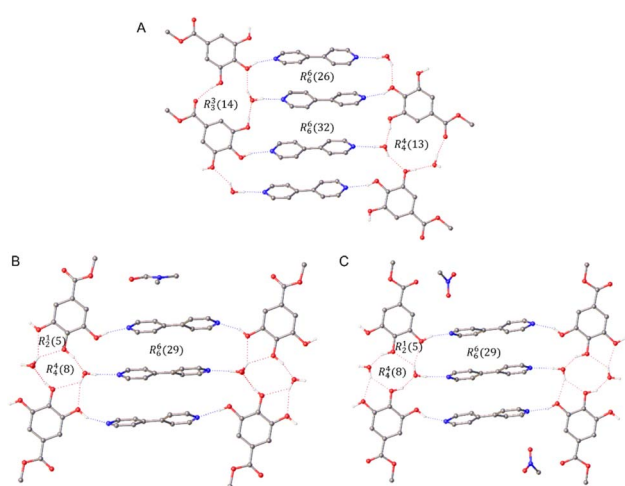

Fig. 3 SCXRD structures showing H-bonding networks in the 4,4'-bipyridine : methyl gallate co-crystal series. (A) 2 : 2 trihydrate, (B) 3 : 2 DMF solvate dihydrate and (C) 3 : 2 MeNO$_2$ disolvate dihydrate.

components would be examined, with new ternary co-crystals to be accessed *via* a shape-size mimicry replacement strategy.

For ternary co-crystal screening, solutions of each of the molecules of interest were prepared in each of four different solvents (MeOH, DMF, MeNO$_2$ and 1,4-dioxane). ENaCt experiments were undertaken using 200 nL of each of the four oils, and 140–150 nL of a solution containing all three components,

in seven different v/v ratios (2 : 1 : 1, 1 : 2 : 1, 1 : 1 : 2, 2 : 2 : 1, 2 : 1 : 2, 1 : 2 : 2 (140 nL), and 1 : 1 : 1 (150 nL); ESI, S3.2.3†).

To validate our methodology, 4 known ternary co-crystals were targeted. Following 288 ENaCt experiments covering 140 crystallisation conditions per target system, for a total of 1152 crystallisations, all four of the desired ternary co-crystals were accessed, and structures obtained by SCXRD. This included toluic acid 10 : isonicotinamide 11 : 3,5-dinitrobenzoic acid 5,[24b] 4,4'-bipyridine 1 : orcinol 12 : phenazine 13,[29] nicotinamide 3 :
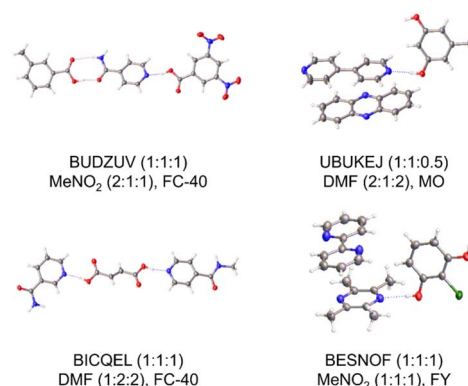

Fig. 4 Previously known ternary co-crystals obtained *via* HOC ENaCt screening. CSD refcode, crystal composition (A/B/C), and ENaCt crystallisation conditions (solvent, v/v/v ratio, oil) shown (MO = mineral oil, PDMSO = poly(dimethylsiloxane), FY = Fomblin YR-1800, and FC-40: Fluorinert FC-40).

fumaric acid **14** : isoniazid **15**,[33] and tetramethylpyrazine **16** : 2,2′-bipyridine **17** : 2-chlororesorcinol **18** (Fig. 4).[34]

As a by-product of our search for known ternary co-crystals, a number of other systems were identified by SCXRD, including single component crystals as well as binary and ternary co-crystals (ESI, S4.4.1†). Of particular note was the serendipitous discovery of a new (1 : 0.5 : 1) ternary co-crystal of tetramethylpyrazine **16** : 2,2′-bipyridine **17** : 2-chlororesorcinol **18**, showing an alternative stoichiometry to that previously known (Fig. 5).

Additionally, during the search for a 4,4′-bipyridine **1** : orcinol **12** : phenazine **13** ternary system, serendipitous discovery of two binary co-crystals were obtained, a known 1.5 : 1 4,4′-bipyridine **1** : orcinol **12** co-crystal and a new 1 : 1 : 0.5 orcinol **12** : phenazine **13** : 1,4-dioxane co-crystal solvate (ESI, S4.4.2†).

Our HOC ENaCt screening was next applied to the discovery of new ternary forms. Of our previously investigated binary co-crystal systems, seven contained one molecular species present in two distinct crystallographic environments. These crystal systems were selected as templates for new ternary co-crystals, in which we aimed to replace one of these molecules within the crystal with a suitable isostere, using shape-size mimicry. Structural isosteres were selected manually based on similarities in size, shape, functional group, and functional group orientation. Thus, applying our previously described ternary HOC ENaCt screening approach to these chosen systems, we were successful in designing and accessing 5 new ternary co-crystals in which at least one molecular component of a binary system had been replaced with a newly introduced co-former molecule (Fig. 6). Note known single component crystals and binary co-crystals were also identified (ESI, S4.4.2†).

Our first challenge was to design new ternary co-crystals based on nicotinamide **3**. Starting with the co-crystal of nicotinamide **3** : quinol **9** (2 : 0.5) as a template, we screened benzoic acid **19**, isonicotinamide **11** and nicotinic acid **20** as shape-size mimics for the replacement of a nicotinamide molecule within the crystal structure (ESI, S4.4.2†). Only co-crystallisation with benzoic acid **19** proved successful, forming a ternary co-crystal in which the newly introduced benzoic acid **19** moiety formed an H-bonded dimer with nicotinamide **3**, mimicking the nicotinamide to nicotinamide H-bonded dimer in the parent binary system. In addition, attempted co-crystallisations of nicotinamide **3**, quinol **9** and nicotinic acid **20** gave no ternary co-crystals, but did result in the serendipitous formation of a novel co-crystal polymorph of nicotinamide **3** : quinol **9** (2 : 0.5). We were also able to build on the nicotinamide **3** : 3,5-

dinitrobenzoic acid **5** binary co-crystal, to form both a new 1 : 1 : 1 ternary co-crystal containing nicotinamide **3**, 3,5-dinitrobenzoic acid **5** and glutaric acid **6**, and a new 1 : 1 : 0.5 ternary co-crystal hydrate containing nicotinamide **3**, 3,5-dinitrobenzoic acid **5** and tetramethylpyrazine **16**. In both cases the ternary co-crystals maintained the key nicotinamide **3** to 3,5-dinitrobenzoic acid **5** N–H–O H-bond.

Attempts to generate ternary co-crystals starting from either 4,4′-bipyridine **1** : 3-hydroxy-2-naphthoic acid **7** or 4,4′-bipyridine **1** : glutaric acid **6** proved challenging, the former providing only the previously discussed binary co-crystals (1.5 : 1 and 0.5 : 1 stoichiometries), as well as a novel binary co-crystal 3-hydroxy-2-naphthoic acid **7** : 1,2-bis(4-pyridyl)ethane **21**, (1 : 0.5), whilst the later mainly gave the parent 4,4′-bipyridine **1** : glutaric acid **6** co-crystal (2 : 2), as well as a known 4,4′-bipyridine **1** : 3,3′-thiodipropionic acid **22** (0.5 : 0.5) co-crystal. The 4,4′-bipyridine **1** : methyl gallate **8** system did however allow access to a new 4,4′-bipyridine **1** : methyl gallate **8** : 2-chlororesorcinol **18** (3 : 2 : 1) dihydrate, which maintained the core 4,4′-bipyridine/methyl gallate/water, H-bonded chain structure.

Finally, starting from caffeine **2** : quinol **9** (1 : 1.5), attempts to introduce suitable shape-size mimics for quinol proved unsuccessful, with no new ternary systems obtained. The parent binary co-crystal was observed in almost all cases, with the one exception being the observation of a known binary co-crystal of quinol **9** : tetramethylpyrazine **16** (0.5 : 0.5). The caffeine **2** : 3,5-dinitrobenzoic acid **5** co-crystal proved more successful, resulting in a new ternary co-crystal hydrate of caffeine **2** : 3,5-dinitrobenzoic acid **5** : 2-methylresorcinol **23** (1 : 1 : 2).

Higher order co-crystals – quaternary co-crystals

Following the highly successful generation of new ternary co-crystals *via* ENaCt, next we decided to extend our investigation to encompass more challenging HOCs, quaternary co-crystals.

Based on our ternary screening approach, for quaternary co-crystal screening by ENaCt four different solvents were again used (MeOH, DMF, MeNO$_2$ and 1,4-dioxane) to prepare near saturated solutions of each of the four molecules required for each system. 200 nL of each of the four oils were distributed across standard 96-well glass plates (ESI S3.2.4†), followed by the sequential pick-up of each component solution in a simple 1 : 1 : 1 : 1 volume ratio into the dispensing needles, for a total volume of 140 nL. These solutions were then injected into the pre-prepared oil containing 96-well plates, plates were sealed with a glass coverslip and stored for 2 weeks before being assessed by polarising optical microscopy.

Four known quaternary co-crystal systems were initially targeted to validate the use of ENaCt in such a demanding HOC formation experiment, namely tetramethylpyrazine **16** : phenazine **13** : pyrene **24** : resorcinol **25**,[25a] 2-chlororesorcinol **18** : tetramethylpyrazine **16** : 2,2′-bipyridine **17** : 1,2-bis(4-pyridyl)ethane **21**,[34] 2-bromoresorcinol **26** : tetramethylpyrazine **16** : 2,2′-bipyridine **17** : 1,2-bis(4-pyridyl)ethane **21**,[34] and 2-chlororesorcinol **18** : tetramethylpyrazine **16** : 2,2′-bithiophene **27** : 1,2-bis(4-pyridyl)ethane **21**.[34] In all four cases suitable quaternary
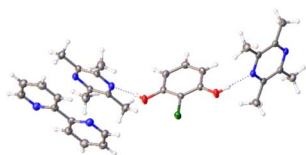

Fig. 5 Serendipitous discovery of a new ternary co-crystal tetramethylpyrazine : 2,2′-bipyridine : 2-chlororesorcinol (1 : 0.5 : 1) *via* HOC ENaCt screening.
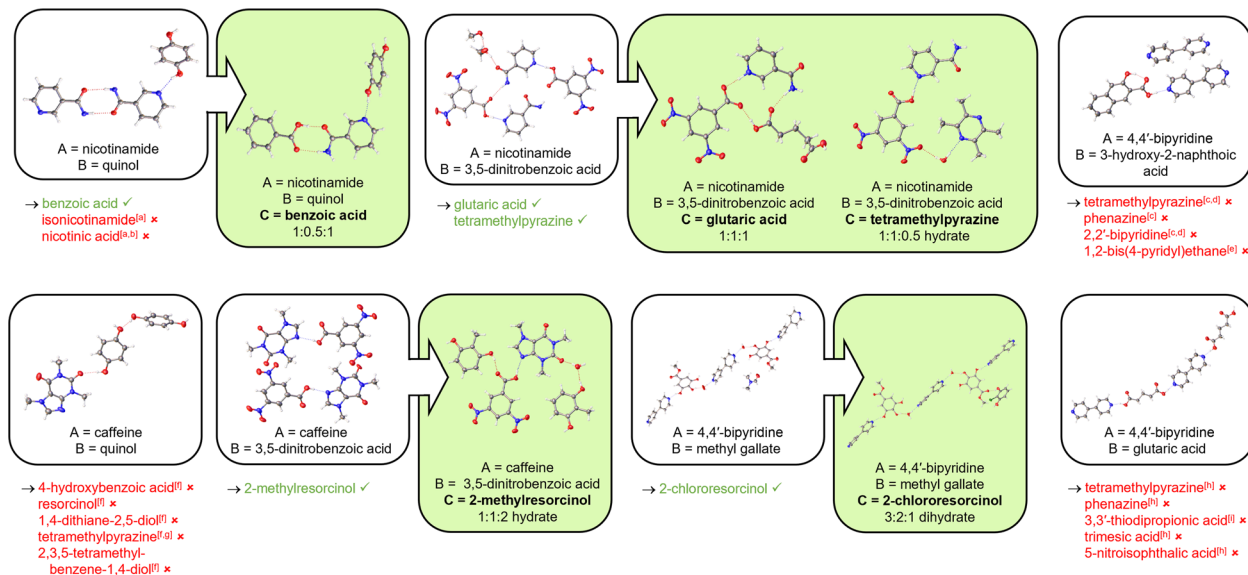
Fig. 6 HOC ENaCt screening outcomes for ternary co-crystal discovery *via* molecular replacement with shape-size mimics from the corresponding binary co-crystals, including parent binary systems (white) and new ternary co-crystals obtained (green). Crystal composition ratio (A/B/C) shown. Co-formers screened are given below each parent binary system, with successful (green) and unsuccessful (red) co-formers highlighted. Additional binary co-crystals obtained are indicated: [a]nicotinamide : quinol (2 : 0.5) polymorph I, [b]nicotinamide : quinol (2 : 0.5) polymorph II, [c]4,4'-bipyridine : 3-hydroxy-2-naphthoic acid (0.5 : 1), [d]4,4'-bipyridine : 3-hydroxy-2-naphthoic acid (1.5 : 1), [e]3-hydroxy-2-naphthoic acid : 1,2-bis(4-pyridyl)ethane (1 : 0.5), [f]caffeine : quinol (1 : 1.5), [g]quinol : tetramethylpyrazine (0.5 : 0.5), [h]4,4'-bipyridine : glutaric acid (2 : 2), [i]4,4'-bipyridine : 3,3'-thiodipropionoic acid (0.5 : 0.5).

co-crystals were grown, and structures obtained by SCXRD (Fig. 7), alongside the observation of known lower order crystals (ESI, 4.4.3†).

Due to the success of applying ENaCt to the formation of known quaternary co-crystals, next we decided to target novel quaternaries *via* this method. To this end we selected several of our previously accessed ternary co-crystal systems (caffeine **2** : 3,5-dinitrobenzoic acid **5** : 2-methylresorcinol **23** hydrate, methyl gallate **8** : 4,4'-bipyridine **1** : 2-chlororesorcinol **18** hydrate, and 2-chlororesorcinol **18** : tetramethylpyrazine **16** :
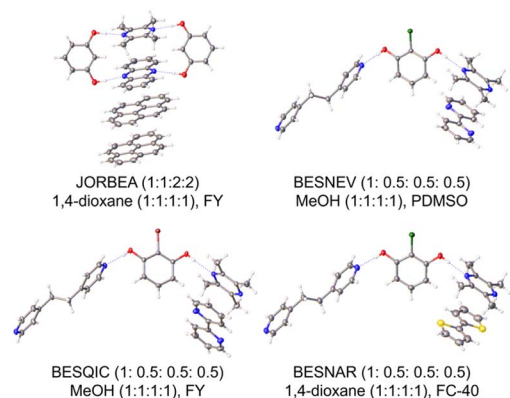

Fig. 7 Previously known quaternary co-crystals obtained *via* HOC ENaCt screening. CSD refcode, crystal composition ratio (A/B/C/D), and ENaCt crystallisation conditions (solvent, v/v/v/v ratio, oil) shown (MO = mineral oil, PDMSO = poly(dimethylsiloxane), FY = Fomblin YR-1800, and FC-40: Fluorinert FC-40).

2,2'-bipyridine **17**), in which at least one component was present in the structure in more than one distinct chemical environment, and engaged in a shape-size mimic screening approach to access new quaternary HOCs, based on our previous success with novel ternary systems.

Starting with the ternary co-crystal system caffeine **2** : 3,5-dinitrobenzoic acid **5** : 2-methylresorcinol **23** hydrate, we targeted the replacement of one of the 2-methylresorcinol **23** moieties, with quinol **9**, orcinol **12**, resorcinol **25**, oxalic acid **28**, 4,4'-dihydroxybiphenyl **29**, 2-bromoresorcinol **26**, 2-chlororesorcinol **18**, 4-chlorobenzene-1,3-diol **30**, 4-bromobenzene-1,3-diol **31** and 4-methylbenzene-1,3-diol **32** (Fig. 8) (ESI, S4.4.3†). Despite the serendipitous discovery of a new ternary co-crystal of caffeine **2** : 2-methylresorcinol **23** : oxalic acid **28** (1 : 1 : 0.5) (Fig. 9A), no quaternary co-crystals were obtained.

The second quaternary system targeted was based on the ternary co-crystal hydrate of methyl gallate **8**, 4,4'-bipyridine **1** and 2-chlororesorcinol **18**. We initially examined the replacement of the 4,4'-bipyridine/H$_2$O complex, thus undertaking ENaCt co-crystallisations with methyl gallate **8**, 4,4'-bipyridine **1** and 2-chlororesorcinol **18** in combination with 1,2-bis(4-pyridyl)ethane **21**, [2,2'-bipyridine]-4,4'-diyldimethanol **33**, [2,2'-bipyridine]-5,5'-dicarboxylic acid **34**, 4,4'-biphenyldimethanol **35**, 4,4'-dihydroxybiphenyl **29**, and 4,4'-biphenyldicarboxylic acid **36** (ESI, S4.4.3†). Unfortunately, none of these experiments yielded new quaternary systems, although three previously observed binary and one previously observed ternary co-crystal were identified, alongside a new binary co-crystal of methyl gallate **8** : [2,2'-bipyridine]-4,4'-diyldimethanol **33** (1 : 0.5) and a new ternary co-crystal of 4,4'-bipyridine **1** : methyl gallate **8** : 2-
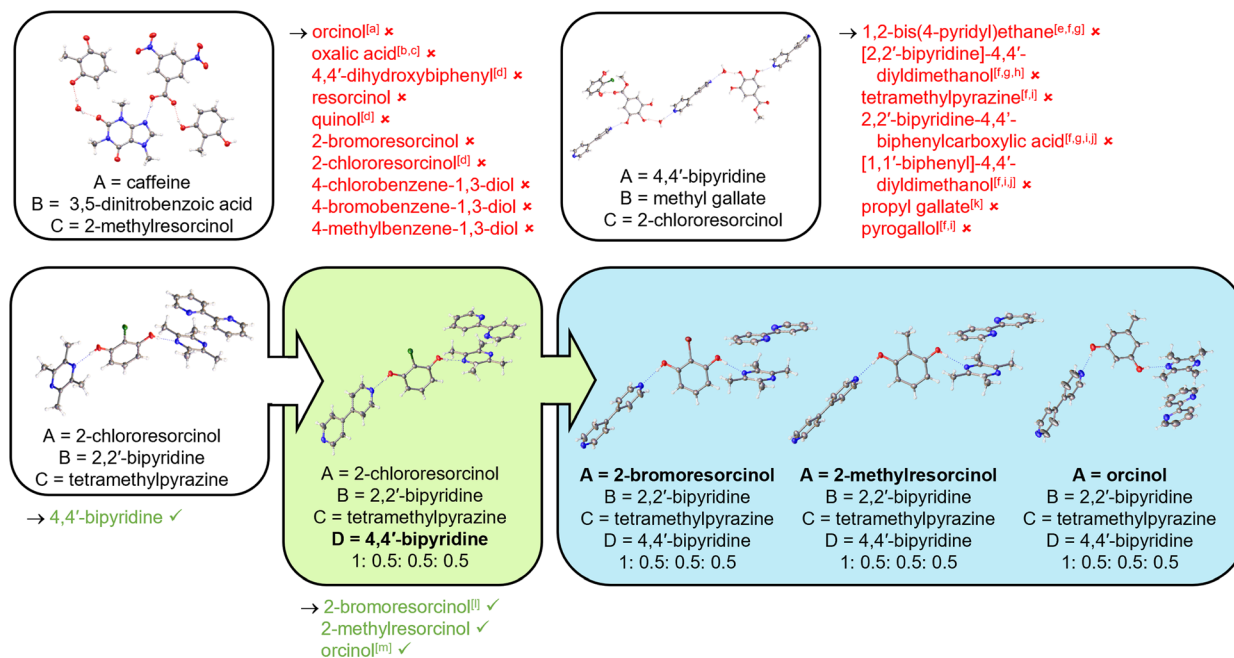
Fig. 8 HOC ENaCt screening outcomes for quaternary co-crystal discovery *via* molecular replacement with shape-size mimics from the corresponding ternary co-crystals, including parent ternary systems (white) and new quaternary co-crystals obtained (green). Crystal composition ratio (A/B/C/D) shown. Co-formers screened are given below each parent ternary system, with successful (green) and unsuccessful (red) co-formers highlighted. Additional binary and ternary co-crystals obtained are indicated: [a]orcinol : 3,5-dinitrobenzoic acid (4 : 4) hydrate, [b]caffeine : oxalic acid (1 : 0.5), [c]caffeine : 2-methylresorcinol : oxalic acid (1 : 1:0.5), [d]caffeine : 3,5-dinitrobenzoic acid : 2-methylresorcinol (1 : 1 : 2) hydrate, [e]4,4′-bipyridine : methyl gallate : 2-chlororesorcinol (3 : 1 : 1), [f]4,4′-bipyridine : methyl gallate (3 : 2) MeNO₂ disolvate dihydrate, [g]4,4′-bipyridine : methyl gallate : 2-chlororesorcinol (3 : 2 : 1) dihydrate, [h]methyl gallate : [2,2′-bipyridine]-4,4′-diyldimethanol (1 : 0.5), [i]4,4′-bipyridine : methyl gallate (2 : 2) trihydrate, [j]4,4′-bipyridine : methyl gallate (3 : 2) DMF solvate dihydrate, [k]4,4′-bipyridine : propyl gallate (1 : 1), [l]2-bromoresorcinol : 4,4′-bipyridine (2 : 3), [m]orcinol : 4,4′-bipyridine (1 : 1.5).
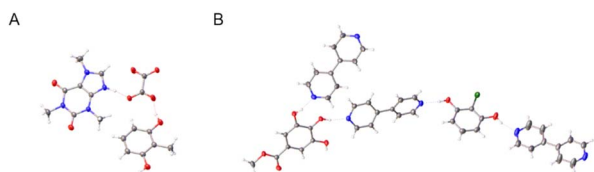

Fig. 9 Serendipitous discovery of new ternary co-crystals (A) caffeine : 2-methylresorcinol : oxalic acid (1 : 1 : 1) and (B) 4,4′-bipyridine : methyl gallate : 2-chlororesorcinol (3 : 1 : 1).

chlororesorcinol **18** (3 : 1 : 1) (Fig. 9B). Additional experiments were undertaken to substitute a methyl gallate moiety, with either propyl gallate **37** or pyrogallol **38**. Again, none of the desired quaternary systems were obtained, but a new binary co-crystal was observed, 4,4′-bipyridine **1**: propyl gallate **37** (1 : 1) (ESI, S4.4.3†).

Finally, starting from 2-chlororesorcinol **18** : tetramethylpyrazine **16** : 2,2′-bipyridine **17**, we targeted the substitution of one tetramethylpyrazine **16**. 4,4′-Bipyridine **1** was chosen as it displays a similar antipodal arrangement of sp² nitrogen H-bond acceptor sites. Pleasingly, ENaCt co-crystallisation screening of 2-chlororesorcinol **18**, tetramethylpyrazine **16**, 2,2′-bipyridine **17** and 4,4′-bipyridine **1** resulted in the discovery of a novel (1 : 0.5 : 0.5 : 0.5) quaternary co-crystal. The newly formed HOC was isostructural with the parent system, with 4,4′-bipyridine **1** replacing one tetramethylpyrazine **16** (Fig. 8).

In previous studies, new HOCs have been accessed through the replacement of 2-chlororesorcinol **18**, employing shape-size mimicry with structurally related diols.[29,31,34] Based on this, our goal was therefore to generate a new family of quaternary co-crystals using our newly discovered quaternary co-crystal as the parent system. Thus, experiments were setup following our standard quaternary co-crystal protocols (ESI, S3.2.4†), in which 2-chlororesorcinol **18** was swapped for 2-bromoresorcinol **26**, 2-methylresorcinol **23**, and orcinol **12**.

Alongside the serendipitous discovery of a new binary co-crystal containing 4,4′-bipyridine **1** : 2-bromoresorcinol **26** (ESI, S4.4.3†), we also obtained three novel quaternary co-crystals (Fig. 8). The new quaternary (1 : 0.5 : 0.5 : 0.5) co-crystals were all isomorphous with the parent system, in each case 2-chlororesorcinol **18** being swapped for the newly introduced diol moiety, 2-bromoresorcinol **26**, 2-methylresorcinol **23**, or orcinol **12**.

Thus, the discovery of a family of four isostructural quaternary co-crystals demonstrates the applicability of HTP methods to the solution of complex crystallisation challenges.

Conclusions

The HTP nature of our herein developed ENaCt co-crystallisation method has allowed us to carry out 13 056 individual crystallisations, using only 0.25–5 μg of each substrate

per experiment. Targeted attempts to access binary co-crystals, as well as ternary and quaternary HOCs, gave excellent success rates for both known and new systems, with the co-crystals generated being suitable for direct SCXRD analysis. ENaCt co-crystallisation screening has thus allowed rapid access to 54 different co-crystals, including 17 new binary, 8 new ternary and 4 new quaternary co-crystals. The rapid, material efficient, HTP generation of such a diverse array of co-crystals clearly demonstrates the power and promise of this methodology for future use in both fundamental research and in the development of pharmaceutically relevant co-crystal systems, heralding a new era of complex, multi-component solid-state experimental space exploration for co-crystal discovery.

Data availability

The data supporting this article have been included as part of the ESI.† CCDC 2372065–2372114, 2428848–2428851 contain the supplementary crystallographic data for this paper. These data can be obtained free of charge from The Cambridge Crystallographic Data Centre *via* **https://www.ccdc.cam.ac.uk/structure**.

Author contributions

The manuscript was written through contributions of all authors. JPM carried out crystallisation experiments, SCXRD analysis, and produced the draft manuscript. PAC, JFMcC, MRP and MJH provided supervision and advice. MRP assisted with SCXRD analysis. MJH produced the final manuscript. All authors have given approval for the final version of the manuscript.

Conflicts of interest

JPM, MJH and MRP and authors of a patent application related to this work.

Acknowledgements

Notes and references

1 (a) A. D. Bond, What Is a Co-Crystal?, *CrystEngComm*, 2007, **9**, 833–834; (b) S. Aitipamula, R. Banerjee, A. K. Bansal, K. Biradha, M. L. Cheney, A. R. Choudhury, G. R. Desiraju, A. G. Dikundwar, R. Dubey, N. Duggirala, P. P. Ghogale, S. Ghosh, P. K. Goswami, N. R. Goud, R. R. K. R. Jetti, P. Karpinski, P. Kaushik, D. Kumar, V. Kumar and B. Moulton, Polymorphs, Salts, and Cocrystals: What's in a Name?, *Cryst. Growth Des.*, 2012, **12**, 2147–2152.
2 (a) M. A. Little, M. E. Briggs, J. T. A. Jones, M. Schmidtmann, T. Hasell, S. Y. Chong, K. E. Jelfs, L. Chen and A. I. Cooper, Trapping Virtual Pores by Crystal Retro-Engineering, *Nat. Chem.*, 2015, **7**, 153–159; (b) H. Jiang, P. Hu, J. Ye, K. K. Zhang, L. Yi, W. Hu and C. Kloc, Tuning of the Degree of Charge Transfer and the Electronic Properties in Organic Binary Compounds by Crystal Engineering: A Perspective, *J. Mater. Chem. C*, 2018, **6**, 1884–1902; (c) L. Sun, Y. Wang, F. Yang, X. Zhang and W. Hu, Cocrystal Engineering: A Collaborative Strategy toward Functional Materials, *Adv. Mater.*, 2019, **31**, 1902328; (d) Y. Huang, Z. Wang, Z. Chen and Q. Zhang, Organic Cocrystals: Beyond Electrical Conductivities and Field-Effect Transistors (FETs), *Angew. Chem., Int. Ed.*, 2019, **58**, 9696–9711; (e) Y. Liu, A. Li, S. Xu, W. Xu, Y. Liu, W. Tian and B. Xu, Reversible Luminescent Switching in an Organic Cocrystal: Multi-Stimuli-Induced Crystal-To-Crystal Phase Transformation, *Angew. Chem., Int. Ed.*, 2020, **59**, 15098–15103; (f) M. Li, B. Hua, H. Liang, J. Liu, L. Shao and F. Huang, Supramolecular Tessellations via Pillar[N]Arenes-Based Exo–Wall Interactions, *J. Am. Chem. Soc.*, 2020, **142**, 20892–20901; (g) G.-H. Ning, P. Cui, I. V. Sazanovich, J. Pegg, Q. Zhu, Z.-F. Pang, R.-J. Wei, M. Towrie, K. E. Jelfs, M. A. Little and A. I. Cooper, Organic Cage Inclusion Crystals Exhibiting Guest-Enhanced Multiphoton Harvesting, *Chem*, 2021, **7**, 3157–3170; (h) Y. Wang, H. Wu, L. O. Jones, M. A. Mosquera, C. L. Stern, G. C. Schatz and J. F. Stoddart, Color-Tunable Upconversion-Emission Switch Based on Cocrystal-To-Cocrystal Transformation, *J. Am. Chem. Soc.*, 2023, **145**, 1855–1865.
3 (a) A. Delori, A. J. Urquhart and I. D. H. Oswald, Supramolecular Hair Dyes: A New Application of Cocrystallization, *CrystEngComm*, 2016, **18**, 5360–5364; (b) O. S. Bushuyev, T. Friščić and C. J. Barrett, Controlling Dichroism of Molecular Crystals by Cocrystallization, *Cryst. Growth Des.*, 2016, **16**, 541–545; (c) E. Sangtani, S. K. Mandal, A. S. Sreelakshmi, P. Munshi and R. G. Gonnade, Salts and Cocrystals of Furosemide with Pyridines: Differences in π-Stacking and Color Polymorphism, *Cryst. Growth Des.*, 2017, **17**, 3071–3087; (d) M. Li, Z. Li, Q. Zhang, B. Peng, B. Zhu, J. Wang, L. Liu and X. Mei, Fine-Tuning the Colors of Natural Pigment Emodin with Superior Stability through Cocrystal Engineering, *Cryst. Growth Des.*, 2018, **18**, 6123–6132.
4 (a) Y. Xiao, C. Wu, L. Zhou, Q. Yin and J. Yang, Cocrystal Engineering Strategy for Sustained Release and Leaching Reduction of Herbicides: A Case Study of Metamitron, *Green Chem.*, 2022, **24**, 8088–8099; (b) Y. Xiao, C. Wu, P. Cui, L. Zhou and Q. Yin, Pursuing Green and Efficient Agriculture from Molecular Assembly: A Review of Solid-State Forms on Agrochemicals, *J. Agric. Food Chem.*, 2023, **71**, 10500–10524; (c) Y. Xiao, C. Wu, S. Feng, K. Chen, L. Zhou and Q. Yin, Temperature-Responsive Cocrystal Engineering for Efficacious Delivery of Poorly Water-Soluble Herbicide, *Cryst. Growth Des.*, 2023, **23**, 8381–8395.
5 (a) O. Bolton and A. J. Matzger, Improved Stability and Smart-Material Functionality Realized in an Energetic Cocrystal, *Angew. Chem., Int. Ed.*, 2011, **50**, 8960–8963; (b) K. B. Landenberger, O. Bolton and A. J. Matzger, Energetic–Energetic Cocrystals of Diacetone Diperoxide (DADP):

Dramatic and Divergent Sensitivity Modifications via Cocrystallization, *J. Am. Chem. Soc.*, 2015, **137**, 5074–5079; (*c*) M. K. Bellas and A. J. Matzger, Peroxosolvate Discovery Method Leads to First Cocrystal with Three Energetic Components, *Chem. Commun.*, 2022, **58**, 8806–8809.

6 (*a*) N. Schultheiss and A. Newman, Pharmaceutical Cocrystals and Their Physicochemical Properties, *Cryst. Growth Des.*, 2009, **9**, 2950–2967; (*b*) N. K. Duggirala, M. L. Perry, Ö. Almarsson and M. J. Zaworotko, Pharmaceutical Cocrystals: Along the Path to Improved Medicines, *Chem. Commun.*, 2016, **52**, 640–655; (*c*) G. Bolla and A. Nangia, Pharmaceutical cocrystals: walking the talk, *Chem. Commun.*, 2016, **52**, 8342–8360; (*d*) S. N. Wong, Y. C. S. Chen, B. Xuan, C. C. Sun and S. F. Chow, Cocrystal Engineering of Pharmaceutical Solids: Therapeutic Potential and Challenges, *CrystEngComm*, 2021, **23**, 7005–7038.

7 M. Karimi-Jafari, L. Padrela, G. M. Walker and D. M. Croker, Creating Cocrystals: A Review of Pharmaceutical Cocrystal Preparation Routes and Applications, *Cryst. Growth Des.*, 2018, **18**, 6370–6387.

8 A. V. Trask, An Overview of Pharmaceutical Cocrystals as Intellectual Property, *Mol. Pharmaceutics*, 2007, **4**, 301–309.

9 (*a*) T. Friščić and W. Jones, Recent Advances in Understanding the Mechanism of Cocrystal Formation via Grinding, *Cryst. Growth Des.*, 2009, **9**, 1621–1637; (*b*) T. Friščić, A. V. Trask, W. Jones and W. D. S. Motherwell, Screening for Inclusion Compounds and Systematic Construction of Three-Component Solids by Liquid-Assisted Grinding, *Angew. Chem., Int. Ed.*, 2006, **45**, 7546–7550; (*c*) L. S. Germann, M. Arhangelskis, M. Etter, R. E. Dinnebier and T. Friščić, Challenging the Ostwald Rule of Stages in Mechanochemical Cocrystallisation, *Chem. Sci.*, 2020, **11**, 10092–10100; (*d*) Z. X. Ng, D. Tan, W. L. Teo, F. León, X. Shi, Y. Sim, Y. Li, R. Ganguly, Y. Zhao, S. Mohamed and F. García, Mechanosynthesis of Higher-Order Cocrystals: Tuning Order, Functionality and Size in Cocrystal Design, *Angew. Chem., Int. Ed.*, 2021, **60**, 17481–17490; (*e*) Y. Yano, H. Kasai, Y. Zheng, E. N. Y. Hisaeda and T. Ono, Multicomponent Crystals with Competing Intermolecular Interactions: In Situ X-Ray Diffraction and Luminescent Features Reveal Multimolecular Assembly under Mechanochemical Conditions, *Angew. Chem., Int. Ed.*, 2022, **61**, e202203853; (*f*) Y. Xiao, C. Wu, X. Hu, K. Chen, L. Qi, P. Cui, L. Zhou and Q. Yin, Mechanochemical Synthesis of Cocrystal: From Mechanism to Application, *Cryst. Growth Des.*, 2023, **23**, 4680–4700.

10 A. Li, S. Li, J. Wang, Y. Chen and M. Lu, Pterostilbene–Nicotinamide Cocrystal: A Case Report of Single Cocrystals Grown from Melt Microdroplets, *Cryst. Growth Des.*, 2023, **23**, 6–10.

11 V. Titapiwatanakun, A. W. Basit and S. Gaisford, A New Method for Producing Pharmaceutical Co-Crystals: Laser Irradiation of Powder Blends, *Cryst. Growth Des.*, 2016, **16**, 3307–3312.

12 D.-K. Bučar and L. R. MacGillivray, Preparation and Reactivity of Nanocrystalline Cocrystals Formed via Sonocrystallization, *J. Am. Chem. Soc.*, 2006, **129**, 32–33.

13 D.-K. Bučar, G. M. Day, I. Halasz, Z. Zhang, J. Sander, D. G. Reid, L. R. MacGillivray, M. J. Duer and W. Jones, The Curious Case of (Caffeine)·(Benzoic Acid): How Heteronuclear Seeding Allowed the Formation of an Elusive Cocrystal, *Chem. Sci.*, 2013, **4**, 4417.

14 (*a*) R. A. Chiarella, R. J. Davey and M. L. Peterson, Making Co-Crystals - The Utility of Ternary Phase Diagrams, *Cryst. Growth Des.*, 2007, **7**, 1223–1226; (*b*) G. R. Desiraju, Crystal Engineering: A Holistic View, *Angew. Chem., Int. Ed.*, 2007, **46**, 8342–8356; (*c*) D.-K. Bučar, Engineering Molecular Crystals: Backbreaking, yet Gratifying, *Cryst. Growth Des.*, 2017, **17**, 2913–2918; (*d*) M. K. Corpinot and D.-K. Bučar, A Practical Guide to the Design of Molecular Crystals, *Cryst. Growth Des.*, 2018, **19**, 1426–1453; (*e*) G. Bolla, B. Sarma and A. K. Nangia, Crystal Engineering of Pharmaceutical Cocrystals in the Discovery and Development of Improved Drugs, *Chem. Rev.*, 2022, **122**, 11514–11603; (*f*) D. Braga, Crystal Engineering: From Promise to Delivery, *Chem. Commun.*, 2023, **59**, 14052–14062.

15 (*a*) G. R. Desiraju, Supramolecular Synthons in Crystal Engineering—A New Organic Synthesis, *Angew. Chem., Int. Ed.*, 1995, **34**, 2311–2327; (*b*) G. R. Desiraju, Crystal Engineering: From Molecule to Crystal, *J. Am. Chem. Soc.*, 2013, **135**, 9952–9967; (*c*) S. Saha and G. R. Desiraju, Acid···Amide Supramolecular Synthon in Cocrystals: From Spectroscopic Detection to Property Engineering, *J. Am. Chem. Soc.*, 2018, **140**, 6361–6373.

16 (*a*) D. Musumeci, C. A. Hunter, R. Prohens, S. Scuderi and J. F. McCabe, Virtual Cocrystal Screening, *Chem. Sci.*, 2011, **2**, 883–890; (*b*) J.-J. Devogelaer, S. J. T. Brugman, H. Meekes, P. Tinnemans, E. Vlieg and R. de Gelder, Cocrystal Design by Network-Based Link Prediction, *CrystEngComm*, 2019, **21**, 6875–6885; (*c*) J.-J. Devogelaer, H. Meekes, P. Tinnemans, E. Vlieg and R. de Gelder, Co-Crystal Prediction by Artificial Neural Networks, *Angew. Chem., Int. Ed.*, 2020, **132**, 21895–21902; (*d*) Y. Jiang, Z. Yang, J. Guo, H. Li, Y. Liu, Y. Guo, M. Li and X. Pu, Coupling Complementary Strategy to Flexible Graph Neural Network for Quick Discovery of Coformer in Diverse Co-Crystal Materials, *Nat. Commun.*, 2021, **12**, 5950; (*e*) A. Vriza, A. B. Canaj, R. Vismara, L. J. Kershaw, T. D. Manning, M. W. Gaultois, P. A. Wood, V. Kurlin, N. G. Berry, M. S. Dyer and M. J. Rosseinsky, One Class Classification as a Practical Approach for Accelerating π–π Co-Crystal Discovery, *Chem. Sci.*, 2021, **12**, 1702–1719; (*f*) E. J. Wu, A. W. Kelly, L. Iuzzolino, A. Y. Lee and X. Zhu, Unprecedented Packing Polymorphism of Oxindole: An Exploration In-spired by Crystal Structure Prediction, *Angew. Chem., Int. Ed.*, 2024, **63**, e202406214.

17 S. Morissette, Ö. Almarsson, M. L. Peterson, J. F. Remenar, M. J. Read, A. V. Lemmo, S. Ellis, M. J. Cima and C. R. Gardner, High-Throughput Crystallization: Polymorphs, Salts, Co-Crystals and Solvates of

Pharmaceutical Solids, *Adv. Drug Delivery Rev.*, 2004, **56**, 275–300.

18 (*a*) M. Guidetti, R. Hilfiker, M. Kuentz, A. Bauer-Brandl and F. Blatter, Exploring the Cocrystal Landscape of Posaconazole by Combining High-Throughput Screening Experimentation with Computational Chemistry, *Cryst. Growth Des.*, 2022, **23**, 842–852; (*b*) Y. A. Abramov, L. Iuzzolino, Y. Jin, G. York, C.-H. Chen, C. Scott Shultz, Z. Yang, C. Chang, B. Shi, T. Zhou, C. Greenwell, S. Sekharan and A. Y. Lee, Cocrystal Synthesis through Crystal Structure Prediction, *Mol. Pharmaceutics*, 2023, **20**, 3380–3392.

19 (*a*) A. R. Tyler, R. Ragbirsingh, C. J. McMonagle, P. G. Waddell, S. E. Heaps, J. W. Steed, P. Thaw, M. J. Hall and M. R. Probert, Encapsulated Nanodroplet Crystallization of Organic-Soluble Small Molecules, *Chem*, 2020, **6**, 1755–1765; (*b*) J. P. Metherall, R. C. Carroll, S. J. Coles, M. J. Hall and M. R. Probert, Advanced Crystallisation Methods for Small Organic Molecules, *Chem. Soc. Rev.*, 2023, **52**, 1995–2010.

20 (*a*) A. Subeh, A. L. Waldbusser, H. A. Raja, C. J. Pearce, K. L. Ho, M. J. Hall, M. R. Probert, N. H. Oberlies and S. Hematian, Structural Diversity of Perylenequinones Is Driven by Their Redox Behavior, *J. Org. Chem.*, 2022, **87**, 2697–2710; (*b*) J. Zhu, I. Moreno, P. Quinn, D. S. Yufit, L. Song, C. M. Young, Z. Duan, A. R. Tyler, P. G. Waddell, M. J. Hall, M. R. Probert, A. D. Smith and A. C. O'Donoghue, The Role of the Fused Ring in Bicyclic Triazolium Organocatalysts: Kinetic, X-Ray, and DFT Insights, *J. Org. Chem.*, 2022, **87**, 4241–4253; (*c*) M. S. Cooper, L. Zhang, M. Ibrahim, K. Zhang, X. Sun, J. Röske, M. Göhl, M. Brönstrup, J. K. Cowell, L. Sauerhering, S. Becker, L. Vangeel, D. Jochmans, J. Neyts, K. Rox, G. P. Marsh, H. J. Maple and R. Hilgenfeld, Diastereomeric Resolution Yields Highly Potent Inhibitor of SARS-CoV-2 Main Protease, *J. Med. Chem.*, 2022, **65**, 13328–13342; (*d*) H. E. Straker, L. McMillan, L. Mardiana, G. R. Hebberd, E. Watson, P. G. Waddell, M. R. Probert and M. J. Hall, Polymorph Prediction through Observed Structural Isomorphism Leading to a New Crystalline Form of Cannabidiol, *CrystEngComm*, 2023, **25**, 2479–2484; (*e*) Q. Zhu, L. Wei, C. Zhao, H. Qu, B. Liu, T. Fellowes, S. Yang, A. Longcake, M. J. Hall, M. R. Probert, Y. Zhao, A. I. Cooper and M. A. Little, Soft Hydrogen-Bonded Organic Frameworks Constructed Using a Flexible Organic Cage Hinge, *J. Am. Chem. Soc.*, 2023, **145**, 23352–23360.

21 (*a*) D.-K. Bučar, R. F. Henry, X. Lou, R. W. Duerst, L. R. MacGillivray and G. G. Z. Zhang, Cocrystals of Caffeine and Hydroxybenzoic Acids Composed of Multiple Supramolecular Heterosynthons: Screening via Solution-Mediated Phase Transformation and Structural Characterization, *Cryst. Growth Des.*, 2009, **9**, 1932–1943; (*b*) G. S. Suresh Kumar, P. G. Seethalakshmi, N. Bhuvanesh and S. Kumaresan, Cocrystals of Caffeine with Formylphenoxyaliphatic Acids: Syntheses, Structural Characterization, and Biological Activity, *J. Mol. Struct.*, 2013, **1034**, 302–309; (*c*) M. K. Mishra, K. Mishra, A. Narayan, C. M. Reddy and V. R. Vangala, Structural Basis for Mechanical Anisotropy in Polymorphs of a Caffeine–Glutaric Acid Cocrystal, *Cryst. Growth Des.*, 2020, **20**, 6306–6315; (*d*) R. Martin, T. H. Lilley, N. A. Bailey, C. P. Falshaw, E. Haslam, D. Magnolato and M. J. Begley, Polyphenol–Caffeine Complexation, *Chem. Commun.*, 1986, **2**, 105–106; (*e*) R. Thakuria, S. Cherukuvada and A. Nangia, Crystal Structures of Pyrogallol, Its Hydrate, and Stable Multiple Z′ Cocrystals with N-Heterocycles Containing Metastable Conformers of Pyrogallol, *Cryst. Growth Des.*, 2012, **12**, 3944–3953; (*f*) S. Tothadi and A. Phadkule, Does Stoichiometry Matter? Cocrystals of Aliphatic Dicarboxylic Acids with Isonicotinamide: Odd–Even Alternation in Melting Points, *CrystEngComm*, 2019, **21**, 2481–2484; (*g*) D. A. Lorenzo, S. J. K. Forrest and H. A. Sparkes, Crystal Engineering: Co-Crystals of Cinnamic Acid Derivatives with a Pyridyl Derivative Co-Crystallizer, *Acta Crystallogr., Sect. B:Struct. Sci., Cryst. Eng. Mater.*, 2016, **72**, 87–95; (*h*) L. Zhao, V. Raval, N. E. B. Briggs, R. M. Bhardwaj, T. McGlone, I. D. H. Oswald and A. J. Florence, From Discovery to Scale-Up: α-Lipoic Acid : Nicotinamide Co-Crystals in a Continuous Oscillatory Baffled Crystalliser, *CrystEngComm*, 2014, **16**, 5769–5780; (*i*) T.-F. Tan, J. Han, M.-L. Pang, H.-B. Song, Y.-X. Ma and J.-B. Meng, Achiral Benzoic Acid Derivatives as Chiral Cocrystal Building Blocks in Supramolecular Chemistry: Adducts with Organic Amines, *Cryst. Growth Des.*, 2006, **6**, 1186–1193; (*j*) G. Ramon, K. Davies and L. R. Nassimbeni, Structures of Benzoic Acids with Substituted Pyridines and Quinolines: Salt Versus Co-Crystal Formation, *CrystEngComm*, 2014, **16**, 5802–5810; (*k*) Y.-N. Zhang, H.-M. Yin, Y. Zhang, D.-J. Zhang, X. Su and H.-X. Kuang, Preparation of a 1:1 Cocrystal of Genistein with 4,4′-Bipyridine, *J. Cryst. Growth*, 2017, **458**, 103–109; (*l*) D. Braga, G. Palladino, M. Polito, K. Rubini, F. Grepioni, M. R. Chierotti and R. Gobetto, Three Polymorphic Forms of the Co-Crystal 4,4′-Bipyridine/Pimelic Acid and Their Structural, Thermal, and Spectroscopic Characterization, *Chem.–Eur. J.*, 2008, **14**, 10149–10159.

22 L. Fábián, Cambridge Structural Database Analysis of Molecular Complementarity in Cocrystals, *Cryst. Growth Des.*, 2009, **9**, 1436–1443.

23 (*a*) Z. Li and A. J. Matzger, Influence of Coformer Stoichiometric Ratio on Pharmaceutical Cocrystal Dissolution: Three Cocrystals of Carbamazepine/4-Aminobenzoic Acid, *Mol. Pharmaceutics*, 2016, **13**, 990–995; (*b*) M. Li, Y. Liu, L. Shao, B. Hua, M. Wang, H. Liang, N. M. Khashab, J. L. Sessler and F. Huang, Pillararene-Based Variable Stoichiometry Co-Crystallization: A Versatile Approach to Diversified Solid-State Superstructures, *J. Am. Chem. Soc.*, 2023, **145**, 667–675.

24 (*a*) N. A. Mir, R. Dubey and G. R. Desiraju, Strategy and Methodology in the Synthesis of Multicomponent Molecular Solids: The Quest for Higher Cocrystals, *Acc. Chem. Res.*, 2019, **52**, 2210–2220; (*b*) C. B. Aakeröy and

D. J. Salmon, Building Co-Crystals with Molecular Sense and Supramolecular Sensibility, *CrystEngComm*, 2005, **7**, 439–448; (*c*) C. A. Gunawardana and C. B. Aakeröy, Co-Crystal Synthesis: Fact, Fancy, and Great Expectations, *Chem. Commun.*, 2018, **54**, 14047–14060; (*d*) D. E. Boycov, K. V. Drozd, A. N. Manin, A. V. Churakov and G. L. Perlovich, Rational Design of the Carbamazepine Ternary Cocrystals, *Cryst. Growth Des.*, 2024, **24**, 4862–4873.

25 (*a*) M. Paul and G. R. Desiraju, From a Binary to a Quaternary Cocrystal: An Unusual Supramolecular Synthon, *Angew. Chem., Int. Ed.*, 2019, **58**, 12027–12031; (*b*) M. Rajkumar and G. R. Desiraju, Quaternary and Quinary Molecular Solids Based on Structural Inequivalence and Combinatorial Approaches: 2-Nitro-Resorcinol and 4,6-Di-Chloro-Resorcinol, *IUCrJ*, 2021, **8**, 178–185; (*c*) M. Rajkumar, Quaternary Cocrystals of 3,5-Dihydroxybenzoic Acid, *Cryst. Growth Des.*, 2021, **21**, 3547–3553; (*d*) M. R. Ahsan and A. Mukherjee, Ternary and Quaternary Cocrystals of 2,7-Dihydroxynaphthalene: Systematic Design with a Large Synthon Module, *CrystEngComm*, 2022, **24**, 5930–5937; (*e*) S. Roy, R. Gaur, M. Paul, M. Rajkumar and G. R. Desiraju, Synthetic Strategies toward Higher Cocrystals of Some Resorcinols, *Cryst. Growth Des.*, 2022, **22**, 7578–7589.

26 (*a*) P. G. Karamertzanis, A. V. Kazantsev, N. Issa, A. Welch, C. S. Adjiman, C. C. Pantelides and S. L. Price, Can the Formation of Pharmaceutical Cocrystals Be Computationally Predicted? 2. Crystal Structure Prediction, *J. Chem. Theory Comput.*, 2009, **5**, 1432–1448; (*b*) A. M. Reilly, R. I. Cooper, C. S. Adjiman, S. Bhattacharya, A. D. Boese, J. G. Brandenburg, P. J. Bygrave, R. Bylsma, J. E. Campbell, R. Car, D. H. Case, R. Chadha, J. C. Cole, K. Cosburn, H. M. Cuppen, F. Curtis, G. M. Day, Jr R. A. DiS. A. Dzyabchenko and B. P. van Eijck, Report on the Sixth Blind Test of Organic Crystal Structure Prediction Methods, *Acta Crystallogr., Sect. B: Struct. Sci., Cryst. Eng. Mater.*, 2016, **72**, 439–459; (*c*) S. Yang and G. M. Day, Exploration and Optimization in Crystal Structure Prediction: Combining Basin Hopping with Quasi-Random Sampling, *J. Chem. Theory Comput.*, 2021, **17**, 1988–1999; (*d*) J.-J. Devogelaer, H. Meekes, P. Tinnemans, E. Vlieg and R. de Gelder, Co-Crystal Prediction by Artificial Neural Networks, *Angew. Chem., Int. Ed.*, 2020, **59**, 21711–21718.

27 Ö. Almarsson and M. J. Zaworotko, Crystal Engineering of the Composition of Pharmaceutical Phases. Do Pharmaceutical Co-Crystals Represent a New Path to Improved Medicines?, *Chem. Commun.*, 2004, **17**, 1889–1896.

28 C. B. Aakeröy, A. M. Beatty and B. A. Helfrich, "Total Synthesis" Supramolecular Style: Design and Hydrogen-Bond-Directed Assembly of Ternary Supermolecules, *Angew. Chem., Int. Ed.*, 2001, **40**, 3240–3242.

29 S. Tothadi, A. Mukherjee and G. R. Desiraju, Shape and Size Mimicry in the Design of Ternary Molecular Solids: Towards a Robust Strategy for Crystal Engineering, *Chem. Commun.*, 2011, **47**, 12080–12082.

30 R. Dubey, N. A. Mir and G. R. Desiraju, Quaternary Cocrystals: Combinatorial Synthetic Strategies Based on Long-Range Synthon Aufbau Modules (LSAM), *IUCrJ*, 2016, **3**, 102–107.

31 N. A. Mir, R. Dubey and G. R. Desiraju, Four- and Five-Component Molecular Solids: Crystal Engineering Strategies Based on Structural Inequivalence, *IUCrJ*, 2016, **3**, 96–101.

32 (*a*) R. Dubey and G. R. Desiraju, Combinatorial Selection of Molecular Conformations and Supramolecular Synthons in Quercetin Cocrystal Landscapes: A Route to Ternary Solids, *IUCrJ*, 2015, **2**, 402–408; (*b*) N. A. Mir, R. Dubey, S. Tothadi and G. R. Desiraju, Combinatorial Crystal Synthesis of Ternary Solids Based on 2-Methylresorcinol, *CrystEngComm*, 2015, **17**, 7866–7869; (*c*) R. Dubey and G. R. Desiraju, Combinatorial Crystal Synthesis: Structural Landscape of Phloroglucinol:1,2-Bis(4-Pyridyl)Ethylene and Phloroglucinol:Phenazine, *Angew. Chem., Int. Ed.*, 2014, **53**, 13178–13182.

33 S. Aitipamula, A. B. H. Wong, P. S. Chow and R. B. H. Tan, Novel Solid Forms of the Anti-Tuberculosis Drug, Isoniazid: Ternary and Polymorphic Cocrystals, *CrystEngComm*, 2013, **15**, 5877–5887.

34 M. Paul, S. Chakraborty and G. R. Desiraju, Six-Component Molecular Solids: $ABC[D_{1-(x+y)}E_xF_y]_2$, *J. Am. Chem. Soc.*, 2018, **140**, 2309–2315.